Chapter 2

# High-Temperature Oxidation of Superalloy C-263 of Rings for Aircraft Engines

Citlalli Gaona Tiburcio, Alejandro Lira Martinez,
Jorge Taboada Solis, Patricia Zambrano Robledo,
Francisco Estupiñán López,
Jose Cabral Miramontes and
Facunda Almeraya Calderón

Additional information is available at the end of the chapter

http://dx.doi.org/10.5772/intechopen.70256

**Abstract**

The present investigation was conducted to study the oxidation kinetics of nickel-based superalloy 263, used in the manufacture of rings for aircraft engines. For carrying out this study, we first conducted microstructural characterization of the pieces using the techniques of optical microscopy, scanning electronic microscopy, and X-ray diffraction. Subsequently, using the thermogravimetric analysis, the kinetic oxidation of the metal was performed in a temperature range between 700 and 1000°C, using atmospheres of $O_2$. The results of the micrographs show the formation of a protective oxide film on the surface of the material in different oxidizing agents. Finally, it was found that the kinetics of high-temperature oxidation of the superalloy C-263 obeys the parabolic rate law.

**Keywords:** superalloys, oxidation, thermogravimetric, aircraft engines

## 1. Introduction

In order to meet the current demand for the aerospace industry, the production of advanced materials is required that ensure the design and manufacture of a robust product and that meet customer expectations, increased engine performance for fuel efficiency, mechanical strength of the components, and at the same time be lighter and less expensive. Therefore, there is a great interest in the development and study of superalloys that will generate

mechanically resistant aircraft, capable of withstanding corrosive environments at high temperatures. Inside a combustion chamber at duty, on a gas turbine engine of aircraft, very aggressive corrosive agents exist. One of these is sulfur, which can deteriorate the materials and reduce their useful life [1].

Nickel-based superalloys are generally used at temperatures above 540°C in very aggressive environments. Seamless rolled rings are made of superalloy Haynes C-230 or C-263 and used in the combustion chamber of gas turbine engines, which are exposed to corrosive gas mixtures. One of those gases is $SO_2$. However, because of its machining process, its corrosion-resistant properties may be compromised [2, 3].

Sulfur is generally present as an impurity in fuels and air. When combustion takes place with excess of air to ensure complete combustion of fuel, sulfur reacts with oxygen to form mainly $SO_2$, which is a corrosive gas. However, sulfidation in oxidizing environments is frequently accelerated by other impurities such as sodium, potassium, and chlorine, making possible the so-called hot corrosion mechanism [4].

Superalloys exposed in $SO_2$ environments generally form oxides and/or sulfides as corrosion products, which depend strongly on temperature. The highest corrosion rate is normally related to the formation of sulfides [1]. Sulfides provide paths for rapid outward diffusion of metals resulting in rapid corrosion attack. For nickel, the corrosion rate in this environment is around 600°C, and above 800°C, the rate decreases with increasing temperature.

Haynes 263 is a nickel-chromium-tungsten-molybdenum alloy that combines high-temperature strength, resistance to oxidizing environments up to 1149°C for prolonged exposures, premier resistance to nitriding environments, and excellent long-term thermal stability [5].

The manufacturing process for forging rings [6] of superalloys may be used in turboreactors or components of the high-temperature section of a gas turbine such as the combustion chambers of the intermediate-temperature section (**Figure 1**) [7].

**Figure 1.** Seamless rolled rings for aircraft engines [6].

http://dx.doi.org/10.5772/intechopen.70256

There are a large number of nickel-based superalloys in the world such as the C-263 which contains multiple phases, depending on the alloying elements. The most prevalent phase in this superalloy is the gamma ($\gamma$) phase, with a cubic crystalline structure centered on the faces. Ni-based superalloys are hardened, due to the formation of solid solutions, using a variety of substitution alloying elements in the $\gamma$-structure such as molybdenum. In the case of superalloy C-263, aluminum and titanium only make up about 3% of the total composition. However, these components are important for the properties of the materials associated with superalloys, due to the formation of the $\gamma'$-phase [8].

In metallic corrosion, the oxidation of alloys at high temperatures can be treated as a special case, which considers the material destruction due to chemical causes, in which solid phases interact either with a liquid agent or a gaseous agent. The latter case involves reducing and oxidizing gases, steam, and even free oxygen. The oxidation is determined by the internal mobility of the solid phases and mainly diffusion in solid state. It is well known that alloying with chromium improves the oxidation resistance of iron at high temperatures [9].

The principal objective in this research was to study the oxidation kinetics of nickel-based superalloy C-263 in a temperature range of 700–1000°C using atmospheres of $O_2$ for 48 h.

## 2. Experimental procedure

The material used in this research was Haynes C-263 superalloy. The specimens were sections of 4 × 4 × 2.5 mm. The surface of samples was ground using 2000 grade grit paper, rinsed with distilled water, and degreased with acetone [10].

**Figure 2.** Thermogravimetric analyzer TA Instruments.

The oxidation test was performed in a thermogravimetric analyzer TA Instruments Hi Res TGA 2950 (**Figure 2**), for 48 h. Experiments were conducted in gaseous atmosphere of $O_2$–$N_2$ with a flow of 75 ml/min at an interval of temperatures of 700–1100°C (+2°C). For each specimen a weight gain measurement in an electronic microbalance (sensitivity $10^{-6}$ g) was set.

The oxidized samples were analyzed in a scanning electron microscopy (SEM; FEI Nova NanoSEM 200) coupled with an energy-dispersive X-ray spectroscopy (EDS) system, in order to understand the oxidation phenomena in terms of scale morphology and oxidation product distribution.

## 3. Results and discussion

### 3.1. Chemical analyzer

The chemical composition of superalloy C-263, used in the present study, is given in **Table 1**. The chemical analysis was performed using the technique of X-ray fluorescence.

### 3.2. Alloy microstructure

The microstructure of the alloys in the study (**Figure 3**) is composed of an austenitic matrix gamma ($\gamma$) and twins that are typical in this material, with intermetallic precipitates of gamma prima ($\gamma'$). The precipitates in the microstructure are in the form of carbides and some borides, and the grains are regular.

### 3.3. Thermogravimetric analyzer

The kinetic measurements indicated that, in general, the alloys presented a parabolic behavior, according to

$$(\Delta m/A)^2 = K_p(t - t_o) \tag{1}$$

where $(\Delta m/A)$ is the weight gain per unit area; $t$ and $t_o$ are the final and initial time, respectively; and $K_p$ is the parabolic rate constant [11].

The increase in mass gain, higher as temperature increases, is significantly lower as the exposure time increases. This progressive decrease in the rate of oxidation indicates the formation of a compact and well-adhered oxide. According to Wagner's [12] theory, systems subjected to high temperature and controlled by diffusion processes, through the network of the oxide layer, follow an oxidation kinetics described by a parabolic-type equation.

| **Chemical composition (% wt.)** | | | | | | | | | | | |
|---|---|---|---|---|---|---|---|---|---|---|---|
| Material | Ni | Cr | Co | Mo | Ti | Fe | Al | Mn | Si | Cu | C |
| C-263 | 51.80 | 20.20 | 19.90 | 6.00 | 2.30 | 0.69 | 0.60 | 0.62 | 0.40 | 0.19 | 0.05 |

**Table 1.** Chemical composition of superalloy C-263.

http://dx.doi.org/10.5772/intechopen.70256

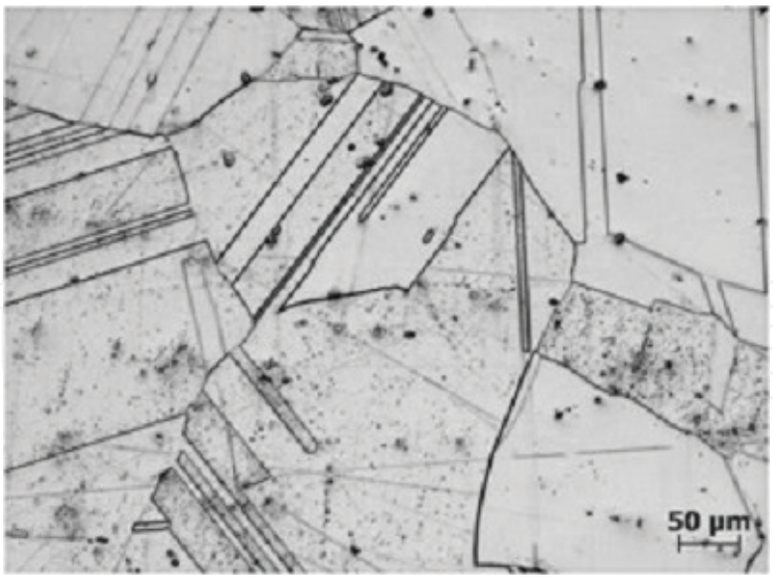


**Figure 3.** Microstructure of superalloy C-263.

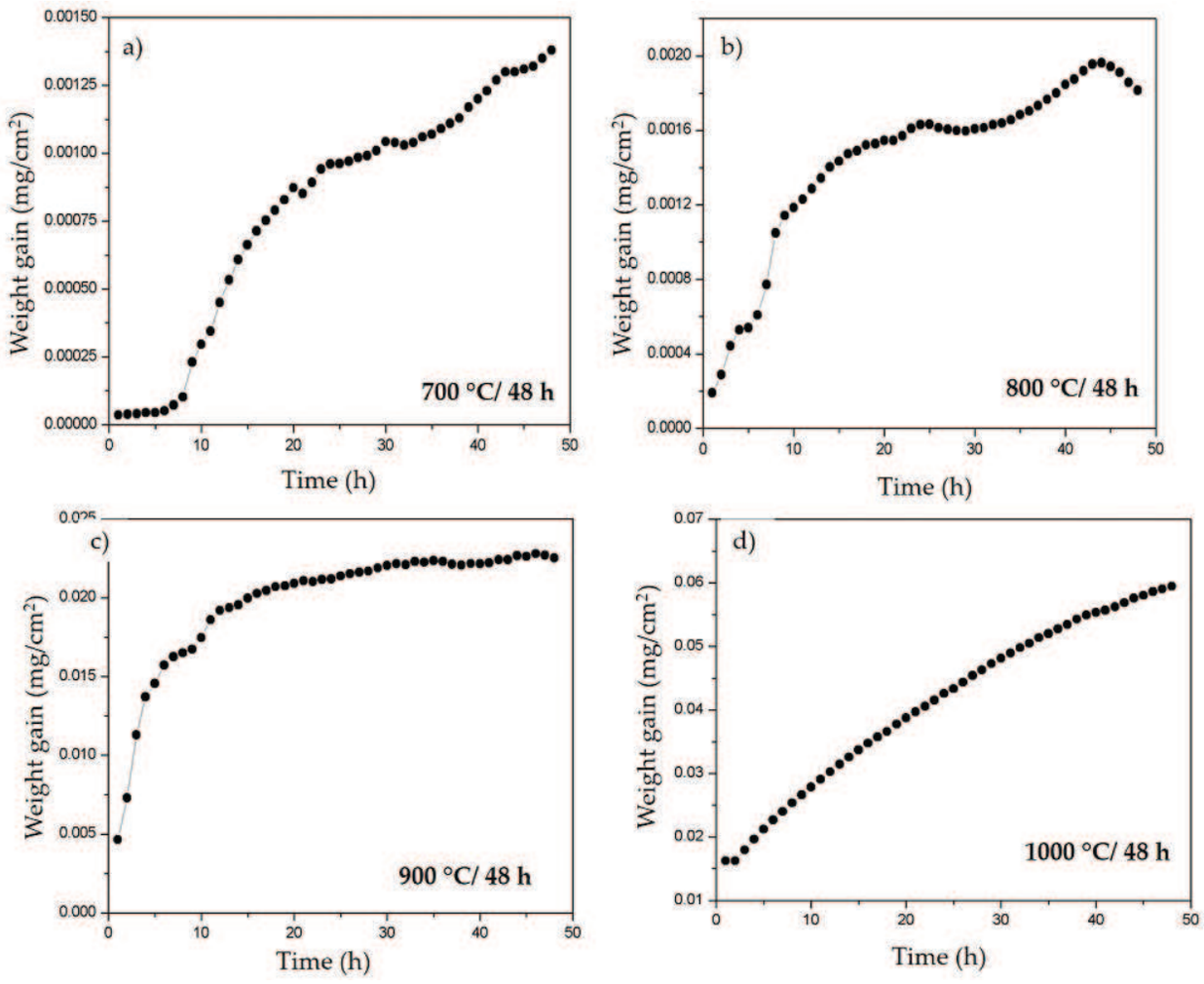


**Figure 4.** Dependence of the weight gain on the oxidation time in $O_2$ at (a) 700°C, (b) 800°C, (c) 900°C, and (d) 1000°C for 48 h.

Oxidation kinetics of superalloy C-263 was studied at 700, 800, 900, and 1000°C; **Figure 4** shows the weight change per unit area versus time. Evidently, the oxidation rate increases as the temperature rises. A parabolic behavior was found at all testing temperatures. The kinetic results are in agreement with those reported in the literature in the sense that the kinetic behavior is parabolic [13, 14].

In order to better visualize this behavior, the square of the mass increase per unit area for superalloy C-263 at the temperatures mentioned above has been plotted in **Figure 5**. For all the cases studied, there is a linear relationship between both variables. This fact confirms that the oxidation of superalloy at the four test temperatures follows a parabolic law. The indicated graphs also allow to calculate the parabolic oxidation rate constants (see **Table 2**).

Knowing the parabolic rate constant for each temperature, the activation energy of the oxidation reaction can be calculated from the Arrhenius equation, which relates $K_p$ to the temperature by the expression:

$$K_{p=} K_o e^{\left(-\frac{Q}{RT}\right)} \tag{2}$$

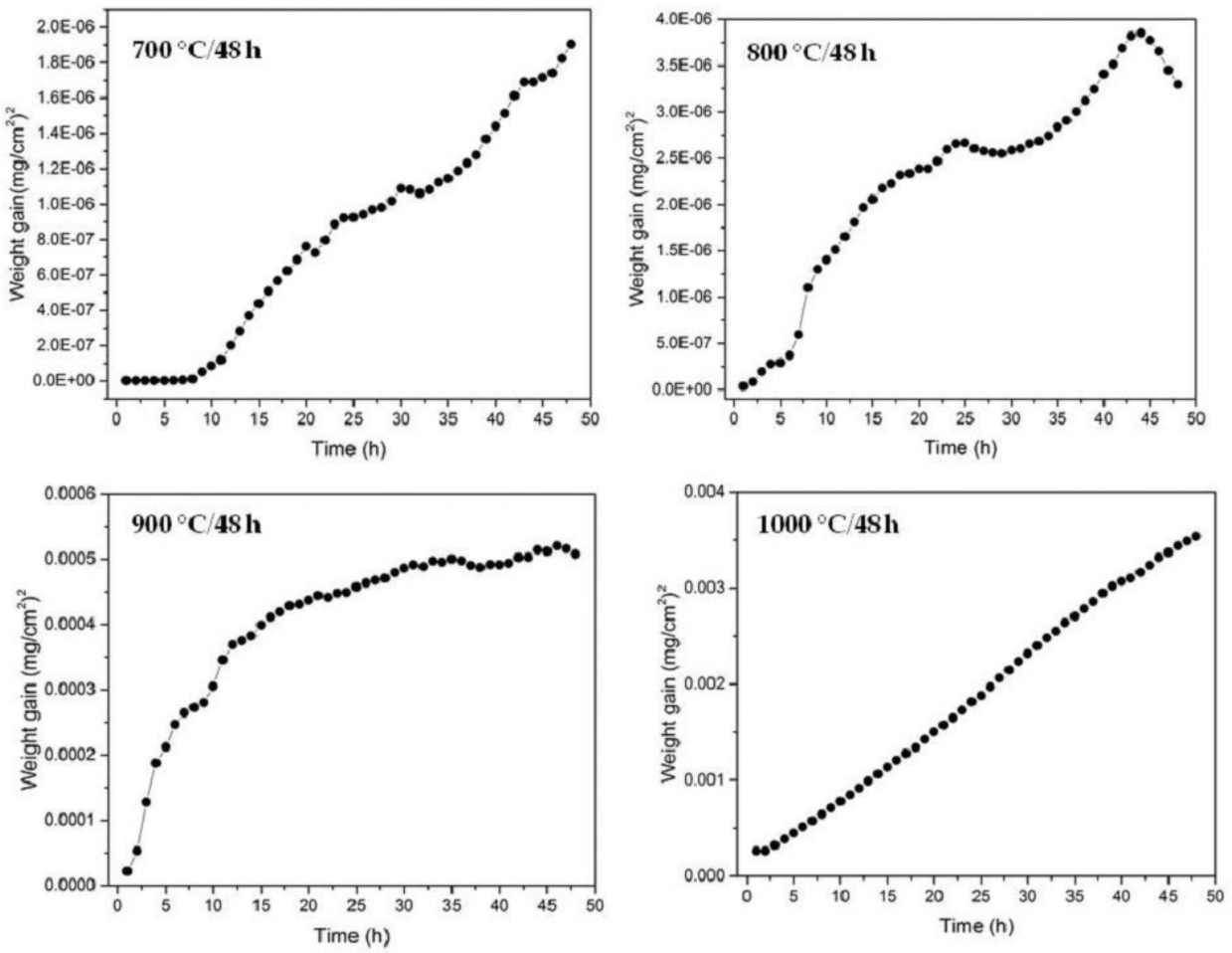


**Figure 5.** Parabolic oxidation of superalloy C-263.

| Temperature (°C) | Parabolic oxidation rate constants ($mg^2/cm^4$ h) |
|---|---|
| 700 | $4.18 \times 10^{-8}$ |
| 800 | $7.21 \times 10^{-8}$ |
| 900 | $7.66 \times 10^{-6}$ |
| 1000 | $7.16 \times 10^{-5}$ |

**Table 2.** Values of the parabolic oxidation rate constant ($mg^2/cm^4$ h).

where $Q$ is the activation energy; $R$ is the gas constant, in joules or calories; $K_o$ is the rate constant at room temperature; and $T$ is the absolute temperature.

In **Figure 6** the parabolic oxidation rate constant is obtained against the inverse of the temperature. The value of the activation energy $Q$ is 28.37 kcal/mol and is indicative that the oxidation process is diffusion controlled through the layer of oxides formed.

The oxide layer in the superalloy samples at 700, 800, and 1000°C remained adherent to the substrate, but not at 900°C, which, after finishing the test, was probably due to the stresses generated with the thermal contraction.

Garcia-Alonso et al. studied the oxidation kinetics of the MA 956 superalloy in the temperature range of 800–1200°C for up to 200 h exposure. During oxidation the alloy develops a fine, compact, and very well-adhered alpha-alumina layer, the thickness of which increases with increasing

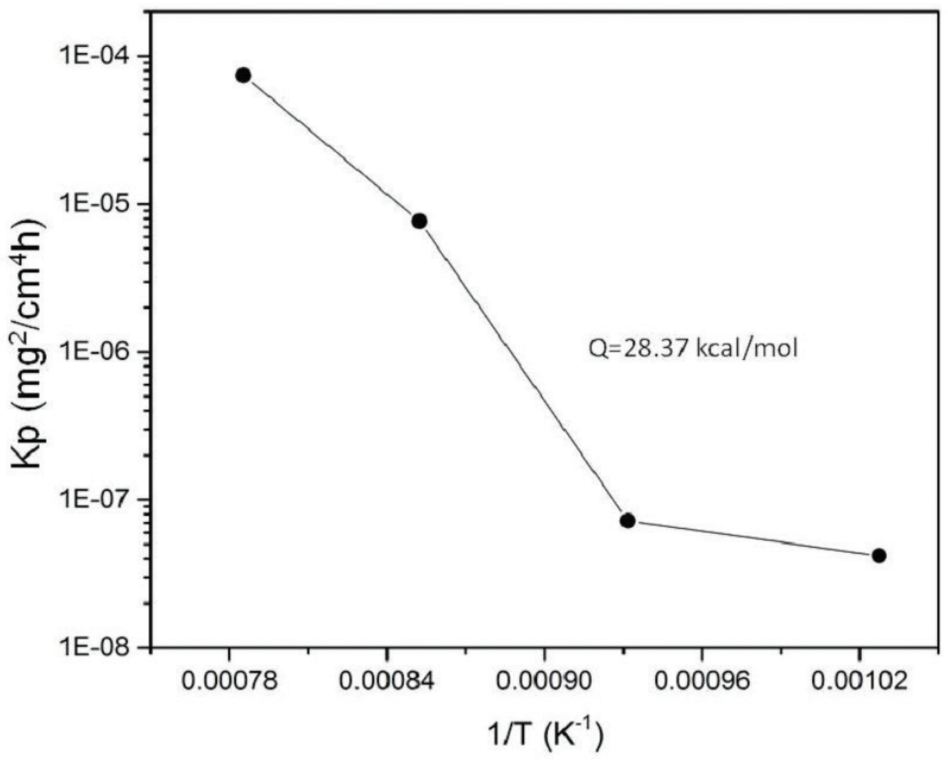


**Figure 6.** Constant of the oxidation rate of superalloy C-263 as a function of temperature.

time and temperature. The oxidation kinetics obeys a subparabolic-type behavior, and the oxidation process would be controlled by alpha-alumina and below 900°C by 7-alumina.

Other authors have studied the behavior of high-temperature oxidation of nickel-based superalloys in different temperature ranges, where the kinetics of oxidation obeys the parabolic law by the addition of elements such as aluminum, titanium, niobium, or yttrium [15, 16].

The Encinas-Oropesa study targeted at characterizing the oxidation behavior of a new nickel-based disk alloy (RR1000) at intermediate temperatures (700–800°C for exposures up to 200 h). The mass gain data obtained have been used to derive oxidation reaction rate parameters, using established methodologies, with parabolic rate constants varying between $1.4 \times 10^{-5}$ $mg^2/cm^4/h$ at 700°C and $8.4 \times 10^{-4}$ $mg^2/cm^4/h$ at 800°C [17].

### 3.4. Scanning electron microscopy (SEM)

The results obtained by SEM on the oxidized specimens revealed different morphologies depending upon the temperature of testing.

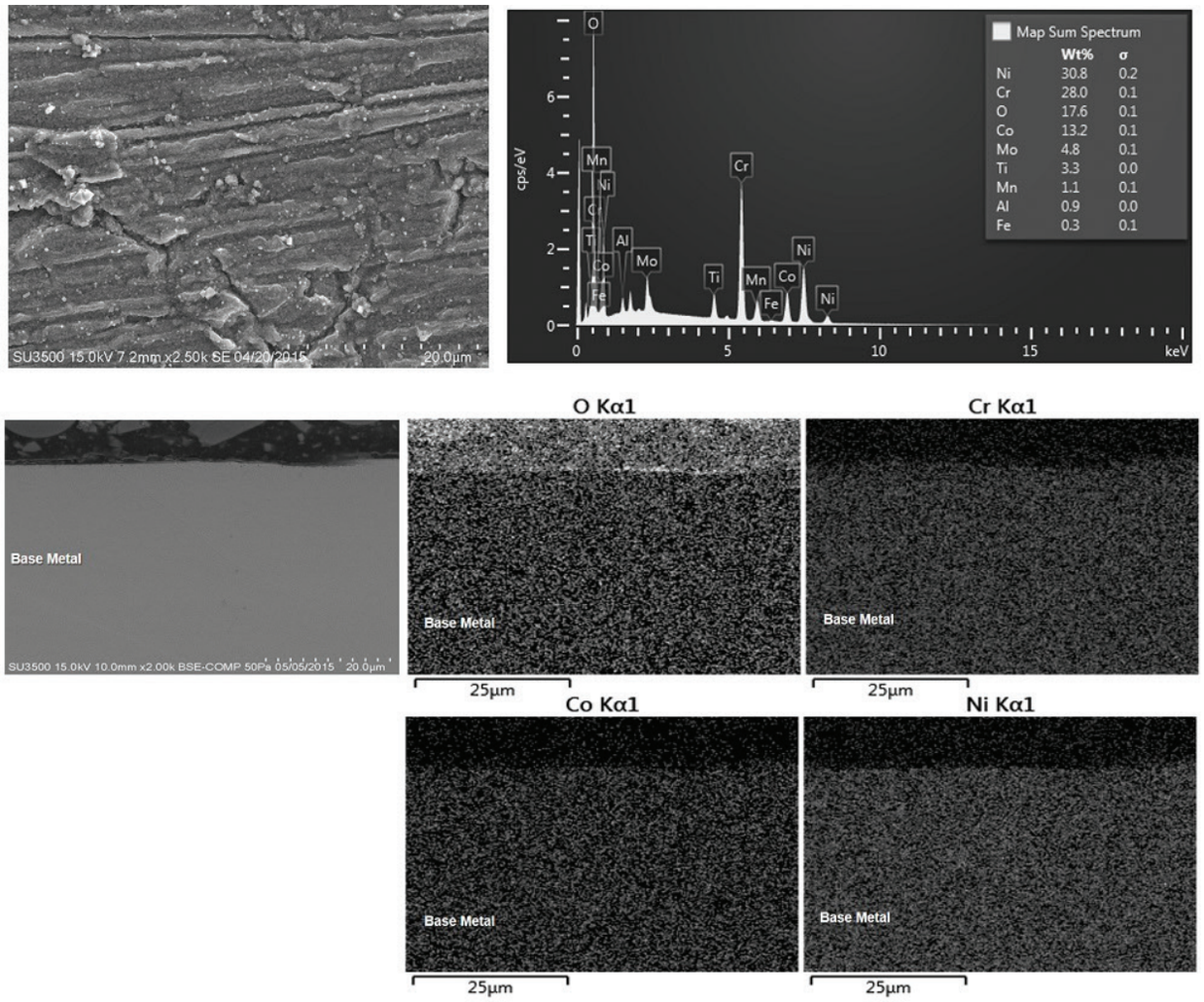


**Figure 7.** Superalloy C-263 at 700°C for 48 h, superficial morphology, cross section, and X-ray map for O, Ni, Co, and Cr.

http://dx.doi.org/10.5772/intechopen.70256

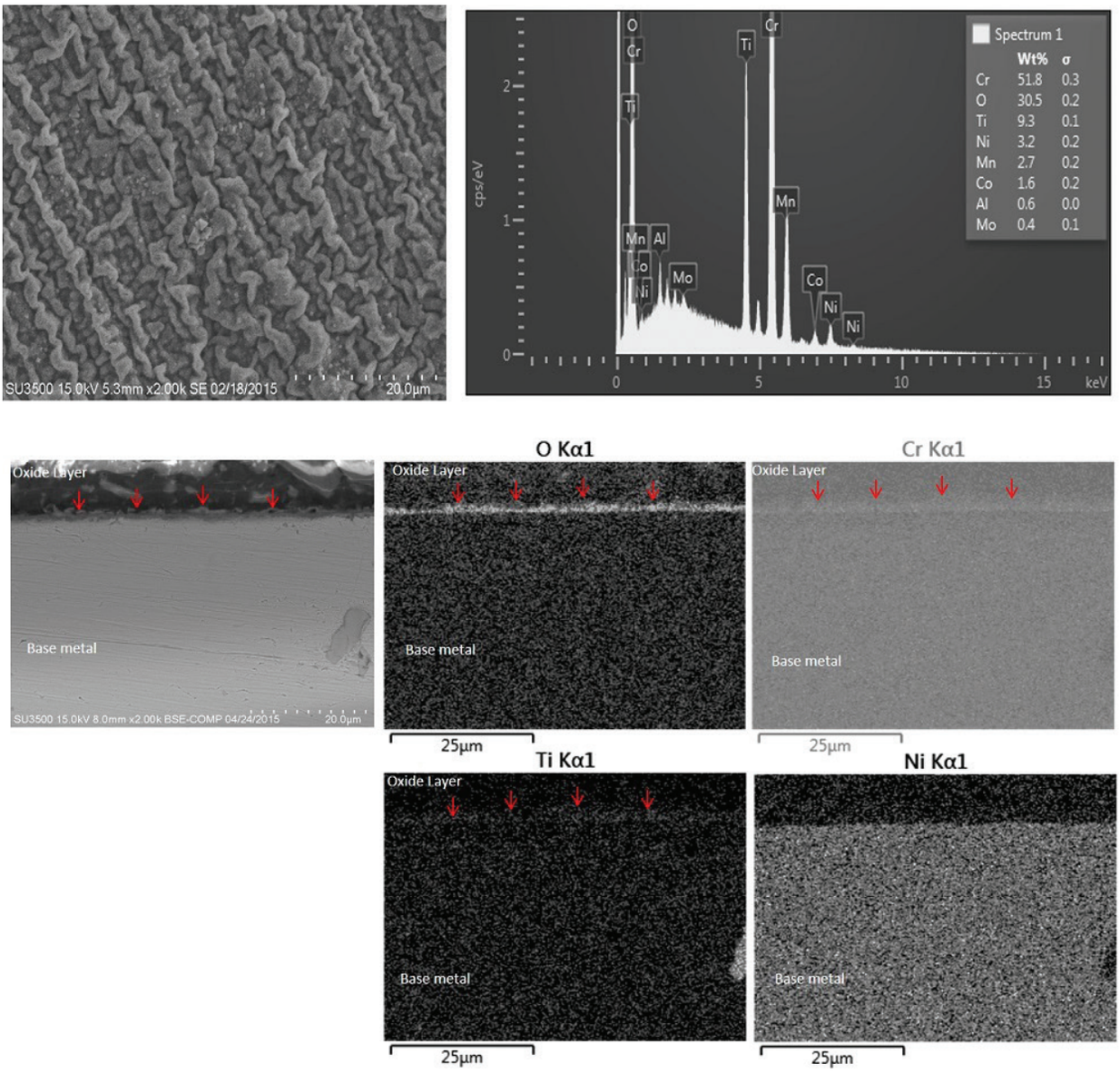


**Figure 8.** Superalloy C-263 at 800°C for 48 h, superficial morphology, cross section, and X-ray map for O, Ni, Ti, and Cr.

The superficial morphology at 700°C presents fine-grained oxides and brittle banded agglomerates (**Figure 7**). Cross-sectional analysis of the samples by SEM/EDS on the layer formed on all alloys suggested the formation of titanium- and chromium-rich oxides.

At 800°C morphology with banded agglomerates, rich in chromium and titanium, is observed; these same elements develop a thin and not very homogeneous layer of chromium oxide and titanium (see X-ray map; **Figure 8**).

Observing the morphology obtained from the superalloy C-263 heat treated at 900°C for 48 h (1000 X), a surface totally covered by a great amount of particles with different sizes and defined morphologies can be noted, although they are more evident those that have form of bars, with larger particle size. **Figure 9** shows the formation of an abundant oxide

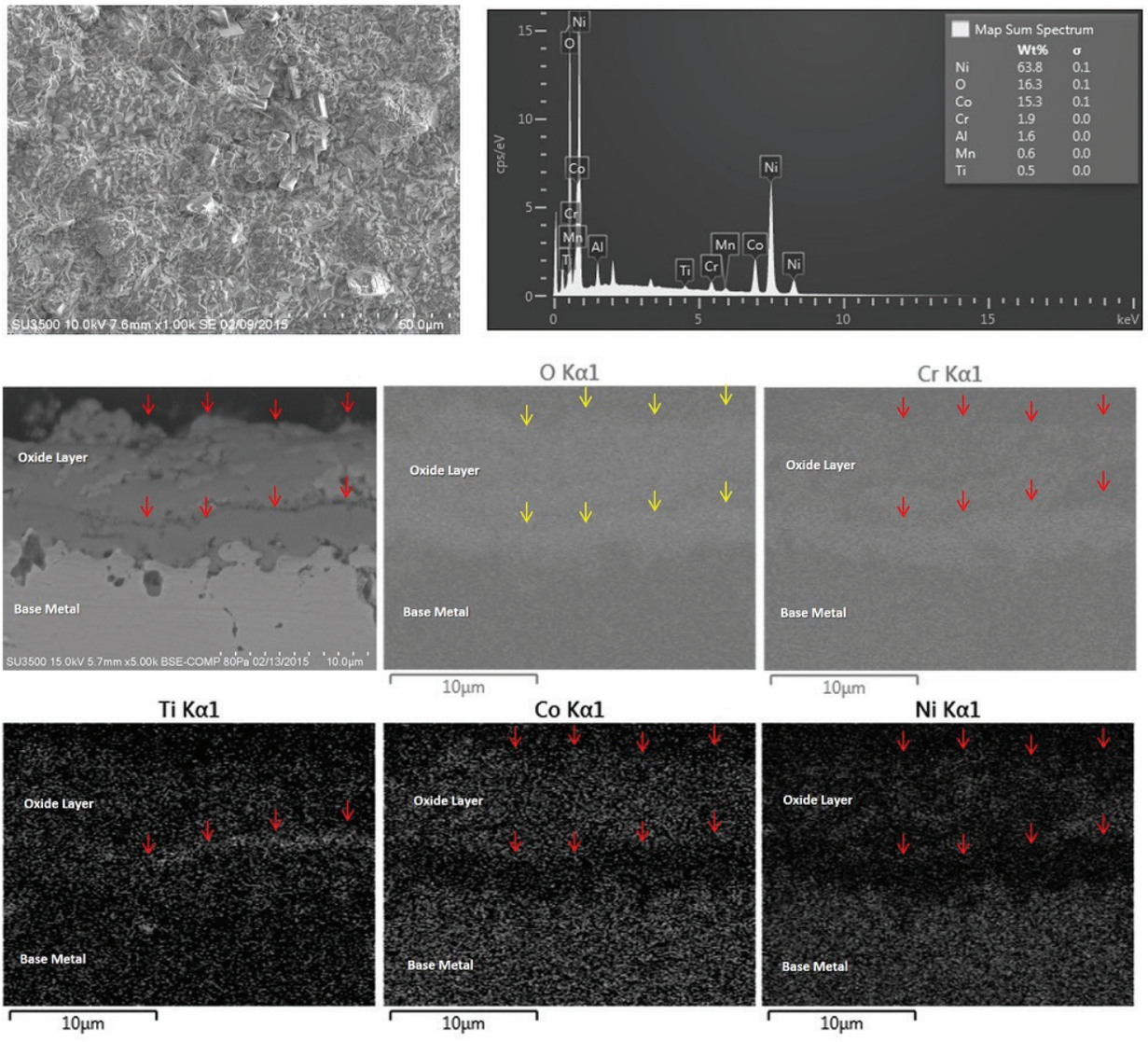


**Figure 9.** Superalloy C-263 at 900°C for 48 h, superficial morphology, cross section, and X-ray map for O, Ni, Co, Ti, and Cr.

layer, in which two layers of oxide, internal and external, can be observed. The inner layer consists mainly of chromium oxide, and the outer layer is formed by an oxide of cobalt and nickel. Between both layers there is an oxide of titanium.

The presence of chromium in this type of superalloys not only improves the mechanical properties by hardening at high temperatures but also stabilizes the phase. Oxidation studies in superalloys with the presence of aluminum and chromium have shown a high tendency of formation of continuous and protective films above 900°C [18–20].

When this superalloy C-263 was treated at 1000°C for 48 h, different morphologies and particle sizes are observed. On the one hand, defined grains with particle sizes between 5 and 10 μm and in some areas the formation of smaller particle agglomerates covering the grains

http://dx.doi.org/10.5772/intechopen.70256

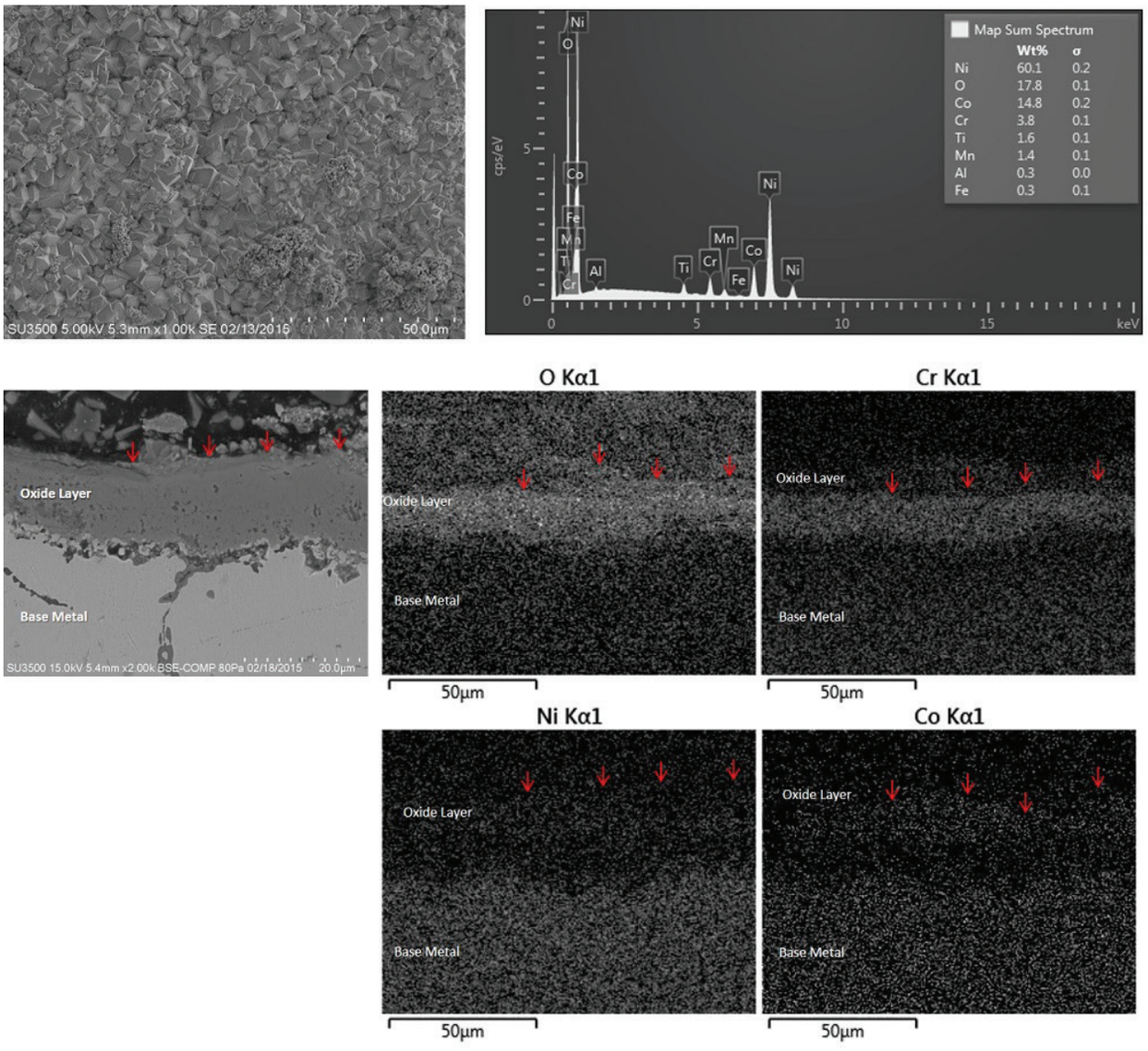


**Figure 10.** Superalloy C-263 at 1000°C for 48 h, superficial morphology, cross section, and X-ray map for O, Ni, Co, Ti, and Cr.

are observed. In X-ray map can be observed, the formation of an abundant oxide layer, in which two layers of oxide, internal and external, is observed; the inner layer is made up mostly of chromium oxide, and the outer layer is formed by a cobalt and nickel oxide (see **Figure 10**; 1000 X).

By SEM-EDS at 800, 900, and 1000°C, the formation of a larger amount of Cr oxide, Ti, and Ni on the surface of superalloy was observed. It was determined that while the temperature of the thermal treatment increased, the amount of the oxide is increased.

The growth rate of $Cr_2O_3$ scales at high temperatures is greatly reduced by the presence of elements as nickel, titanium, and cobalt [21].

## 4. Conclusions

- The kinetics of high-temperature oxidation of the superalloy C-263 obeys the parabolic rate law for temperatures 700, 800, and 1000°C.
- Cross-sectional analysis, by SEM/EDS, of the layer formed on all samples suggested the formation of titanium- and chromium-rich oxides and in some cases cobalt and nickel oxide after 900°C.
- The present investigation found that at 700°C, there is almost no oxide on the surface of the superalloy, only seen a little agglomerates of Mn, Cr, and Ni as major components of the superalloy matrix.

## Author details

Citlalli Gaona Tiburcio[1], Alejandro Lira Martinez[2], Jorge Taboada Solis[1], Patricia Zambrano Robledo[1], Francisco Estupiñán López[1], Jose Cabral Miramontes[1] and Facunda Almeraya Calderón[1]*

*Address all correspondence to: falmeraya.uanl.ciiia@gmail.com

1 Universidad Autónoma de Nuevo León (UANL), Facultad de Ingeniería Mecánica y Eléctrica (FIME), Centro de Investigación e Innovación en Ingeniería Aeronáutica (CIIIA), Av. Universidad s/n. Ciudad Universitaria. San Nicolás de los Garza, Nuevo León, México

2 Universidad Autónoma de Ciudad Juárez, Instituto de Ingeniería y Tecnología, Cd Juárez, Chihuahua, México

## References

[1] Lai GY. High Temperature Corrosion and Materials Applications. 1st ed. USA: ASM International; 2007. p. 345

[2] Rolls R. The Jet Engine. 1st ed. UK: Rolls Royce Technical Publican; 1996. p. 126

[3] Klause H. Jet Engines: Fundamentals of Theory, Design and Operation. 1st ed. Stuttgart, Germany: Motorbooks International Publishers; 2003. p. 345

[4] Stringer J. Hot corrosion in gas turbines. Corrosion. 1972;**28**(5):161

[5] Haynes. Haynes 263 Alloys. 03-02-2015. Available from: http://wwwhayesintl.pdf/h3000.pdf

[6] FRISA. Manufacture Process [Internet]. 02-01-2015. Available from: htto://www.frisa.com/process/manufacturing-process

[7] Pollock T, Tin S. Nickel-based superalloys for advanced turbine engines: Chemistry, microstructure and properties. Journal of Propulsion and Power. 2006;**28**(2):161-374

[8] Pettit F, Meier G. Oxidation and hot corrosion of superalloys. TMS. 1984;**1**:651-687

[9] Seybolt AU. Observations on the Fe-Cr-O System J. Electrochem. Soc. 1960;**107**(3):147-156

[10] ASTM E3-11. Standard Guide for Preparation of Metallographic Specimens. 100 Barrr Harbor Dirve, PO box C700, West Conshohocken, PA, 19428-2959, USA: ASTM International

[11] Saucedo-Acuña RA, Almeraya-Calderón F, De la Torre SD, Martínez-Villafañe A. ICC, editor. Proceedings of the 15th International Corrosion Congress; Granada, España. España: ICC; 2002. p. 570

[12] Wagner C. Atom Movements. ASM; 1951. p. 153

[13] Nakamura Y. Metallurgical Transactions. 1974;**5**:909

[14] Golightly FA, Wood GC, Stott FH. Oxidation Metals. 1980;**14**(3):217

[15] Weng F, Yu H, Chen C. Corrosion Science. 2013;**75**:58-66

[16] Taylor MP, Evans HE, Stekovic S. Surface and Interface Analysis. 2015;**47**(3):362-370

[17] Encinas OA, Simms NJ, Nicholls JR, Hardy MC. Journal Materials at High Temperature. 2009;**26**(3):241-249

[18] Reed RC. The Superalloys Fundamentals and Applications. 1st ed. UK: Cambridge University Press; 2006. p. 390

[19] Moussa SO, Morsi K. Journal of Alloys and Compounds. 2006;**426**(1-2):136-143

[20] Szacalos P, Lundberg M, Pettersson R. Corrosion Science. 2006;**48**(7):1679-1695

[21] Martínez-Villafañe A, Chacón NJ, Gaona TC, Almeraya CF, et al. Materials Science Engineering A. 2003;**A263**:15-19

IntechOpen